NANO MICRO small

Supporting Information

for *Small,* DOI: 10.1002/smll.201602569

Multibuilding Block Janus Synthesized by Seed-Mediated Self-Assembly for Enhanced Photothermal Effects and Colored Brownian Motion in an Optical Trap

*Kanokwan Sansanaphongpricha, Michael C. DeSantis, Hongwei Chen, Wei Cheng, Kai Sun, Bo Wen, and Duxin Sun**

Supporting Information

Multi-Building Block Janus Synthesized by Seed-mediated Self-Assembly for Enhanced Photothermal Effects and Colored Brownian Motion in an Optical Trap

*Kanokwan Sansanaphongpricha, Michael C. DeSantis, Hongwei Chen, Wei Cheng, Kai Sun, Bo Wen, and Duxin Sun**

Materials. Furfuryl alcohol (98%), triethanolamine (TEA, 99%), dioxane (99.5%, extra dry), and1,1,2,2 tetrachloro ethane (TCE,9 8.5%) were purchased from Acros Organics (USA). Petroleum ether (certified ACS grade), and dichloromethane (DCM, certified ACS grade) were purchased from Fisher Scientific (USA). Iron oxide (III) (FeO(OH), hydrated, catalyst grade, 30–50 mesh), oleic acid (technical grade, 90%), 1-octadecene (technical grade, 90%), ethyl acetate (anhydrous, 99.8%), tetrahydrofuran (THF, anhydrous 99.8%), adipoyl chloride, bismaleimido diphenyl methane (BMD), and dimethyl sulfoxide (DMSO, 99.5%) were purchased from Sigma-Aldrich (USA). TCE-d_2, and DCM-d_4 for ^{1}HNMR analysis was purchased from Cambridge Isotope Laboratory (USA). Thiol methoxy polyethylene oxide 5KDa (SH-mPEG) was purchased from NanoCS (USA). Polystyrene-*b*-polyethylene oxide (PS-*b*-PEO), Mw 10,300 Da used as non thermo-cleavable micelles was purchased from Polymer Source (Canada). Dodecanethiol functionalized gold nanoparticles (5nm) were purchased from Nanoprobes (USA).

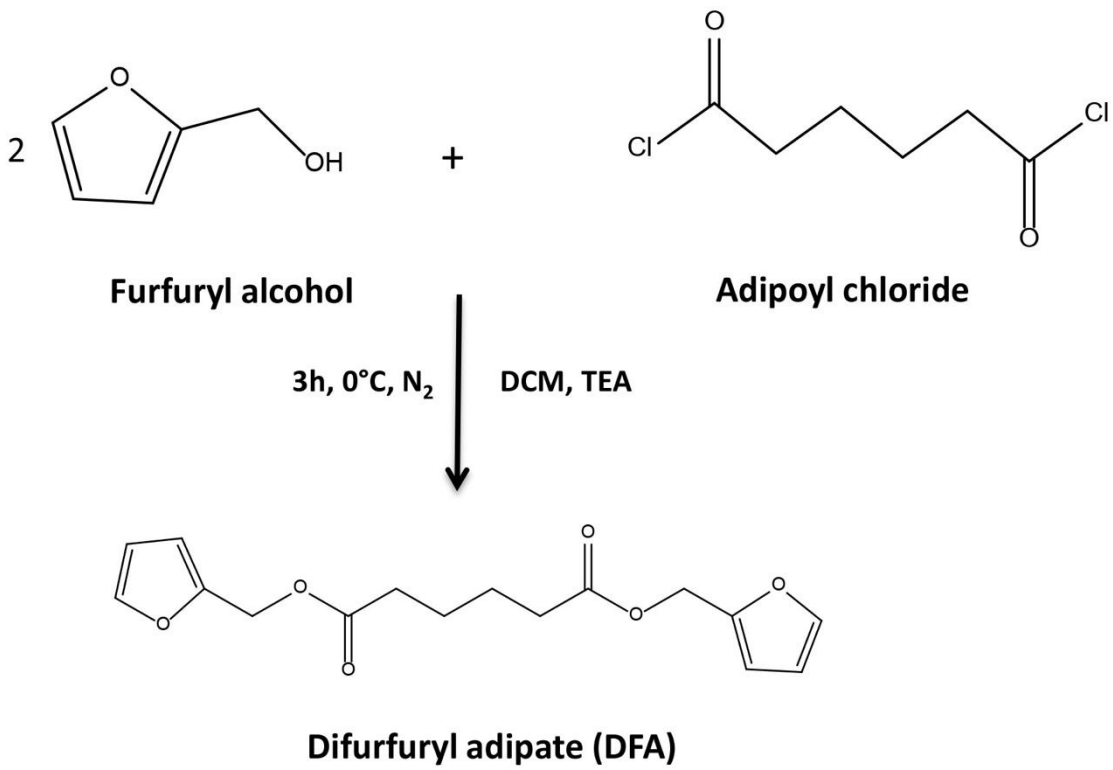

Figure S1. A synthesis scheme of DFA monomer. DFA was synthesized from furfuryl alcohol and adipoyl chloride in DCM with a few drops of TEA under nitrogen atmosphere at 0°C for 3 hours. DFA was characterized by ^{1}H NMR (400 MHz, TCE-d_2) δ 7.43 (d, J = 2.0 Hz, 2H), δ 6.41 (d, J = 2.8Hz, 2H), δ 6.37 (dd, J_1 = 3.6Hz, J_2 = 2.0Hz, 2H), 5.04 (s, 4H), 2.34 (p, J_1 = 7.2 Hz, J_2 = 3.2Hz, 4H), 1.63 (t, J = 3.4 Hz, 4H).

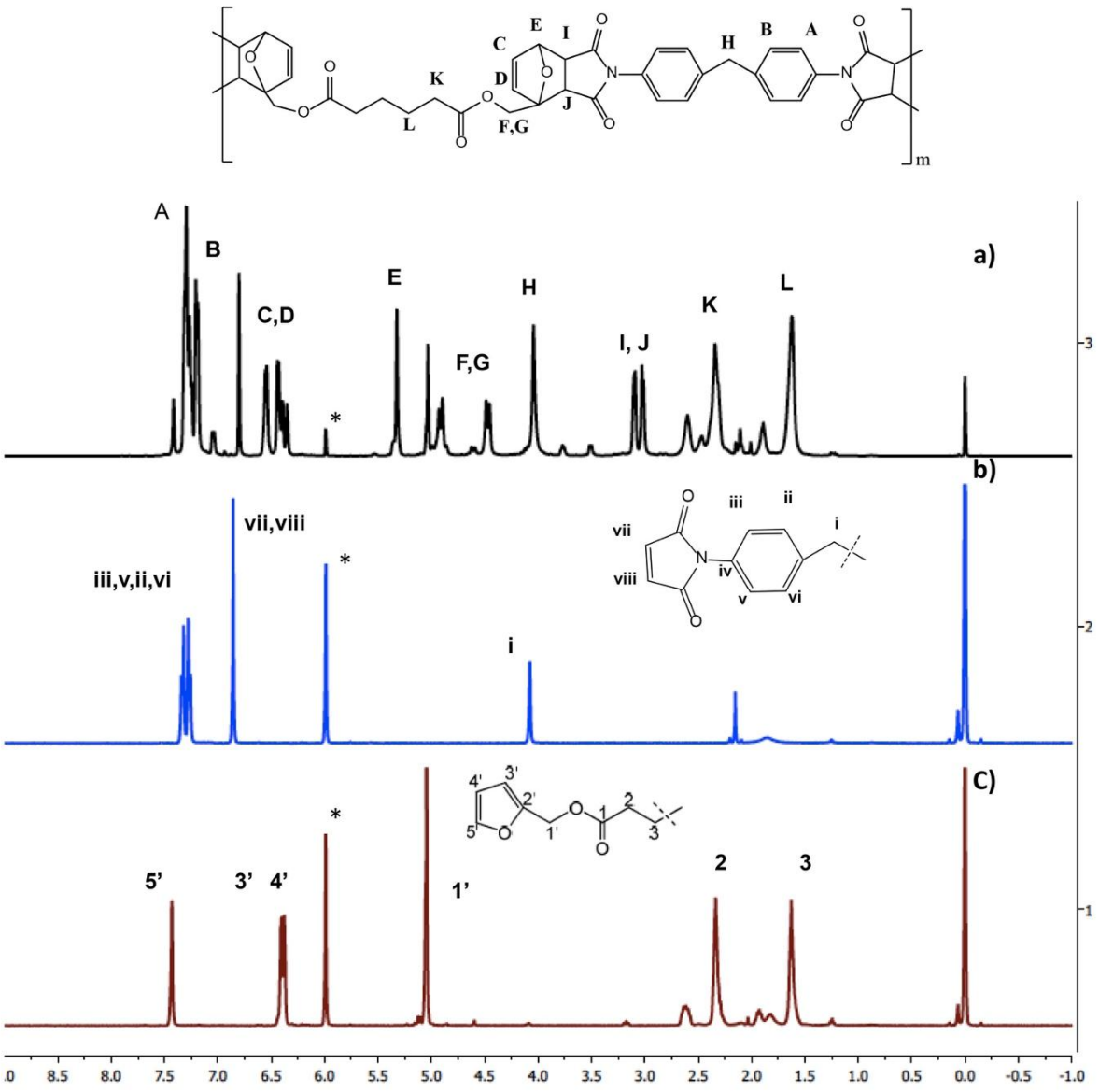

Figure S2. ^{1}H NMR of hydrophobic backbone Diel-Alder polymer (a), bismaleimido diphenyl methane (BMD) (b), and difurfuryl adipate (DFA) (c). BMD and DFA covalently form cycloadducts as shown in ^{1}H NMR at δ 7.30 (d, J = 8 Hz, 4H), δ 7.19 (d, J = 8 Hz, 4H), δ 6.55 (d, J = 6.4 Hz, 2H), δ 6.43 (d, J = 5.6 Hz, 2H), δ 5.32 (s, 2H), δ 4.91 (d, J = 13.2 Hz, 2H), δ 4.47 (d, J = 13.2 Hz, 2H), δ 4.04 (s, 2H), δ 3.09 (d, J = 5.6 Hz, 2H), δ 3.02 (d, J = 6.4 Hz, 2H), δ 2.34 (m, 4H), δ 1.63 (m, 4H). The asterisk (*) indicates a solvent peak.

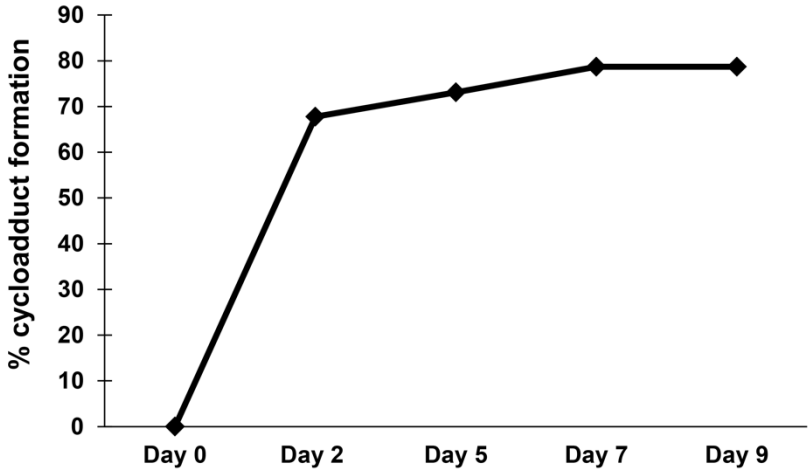

Figure S3. The percent of cycloadduct formation in the polymer was calculated from ^{1}H NMR of hydrophobic backbone Diel-Alder polymer at 5.32 ppm and 7.43 ppm at different time points of polymerization. The polymerization happens quickly at the first 48 hours of the reaction and almost constant after 7 days.

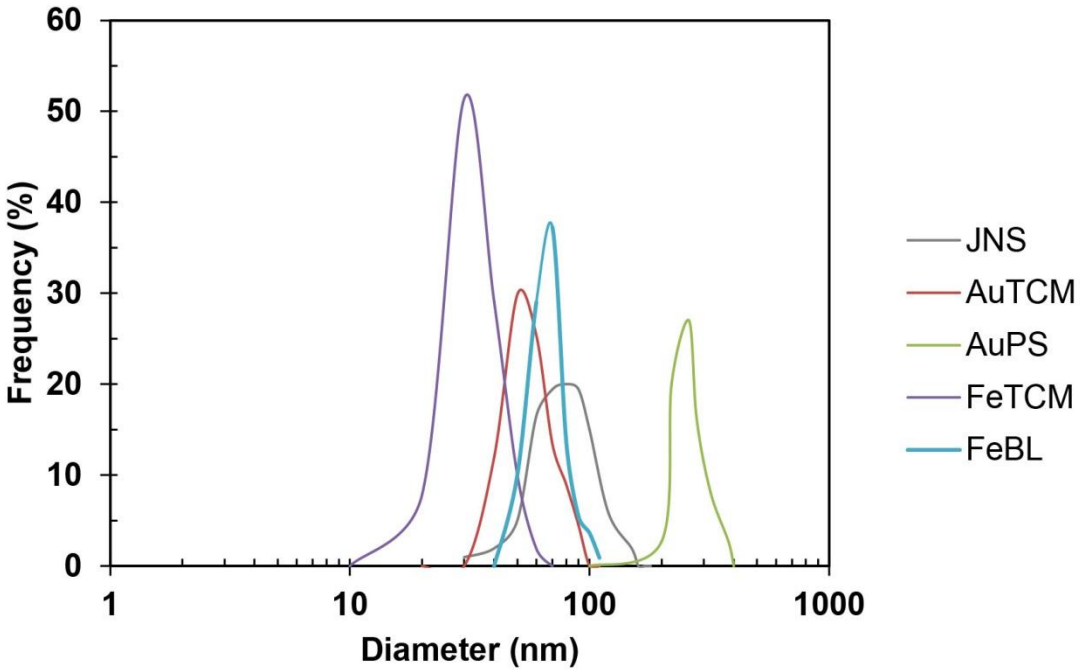

Figure S4. Core diameters and size distributions of JNS, AuTCM, AuPS, FeTCM and FeBL measured by TEM and analyzing by Image J.

	Hydrodynamic Diameter (nm)	Polydispersity index (PDI)
TCM	93.82	0.35
FeTCM	78.82	0.22
AuTCM	94.88	0.24
JNS	100.30	0.12

Table S1. The table shows hydrodynamic diameters and polydispersesity index of TCM seed, FeTCM, AuTCM, and JNS. Each sample was measure in triplicate by using Malvern Zeta sizer with disposable cuvettes. The core diameters of micelles measured by DLS are larger than the diameter of micelles measured by TEM because of the interaction between the media and the polymer coating nanoparticles.

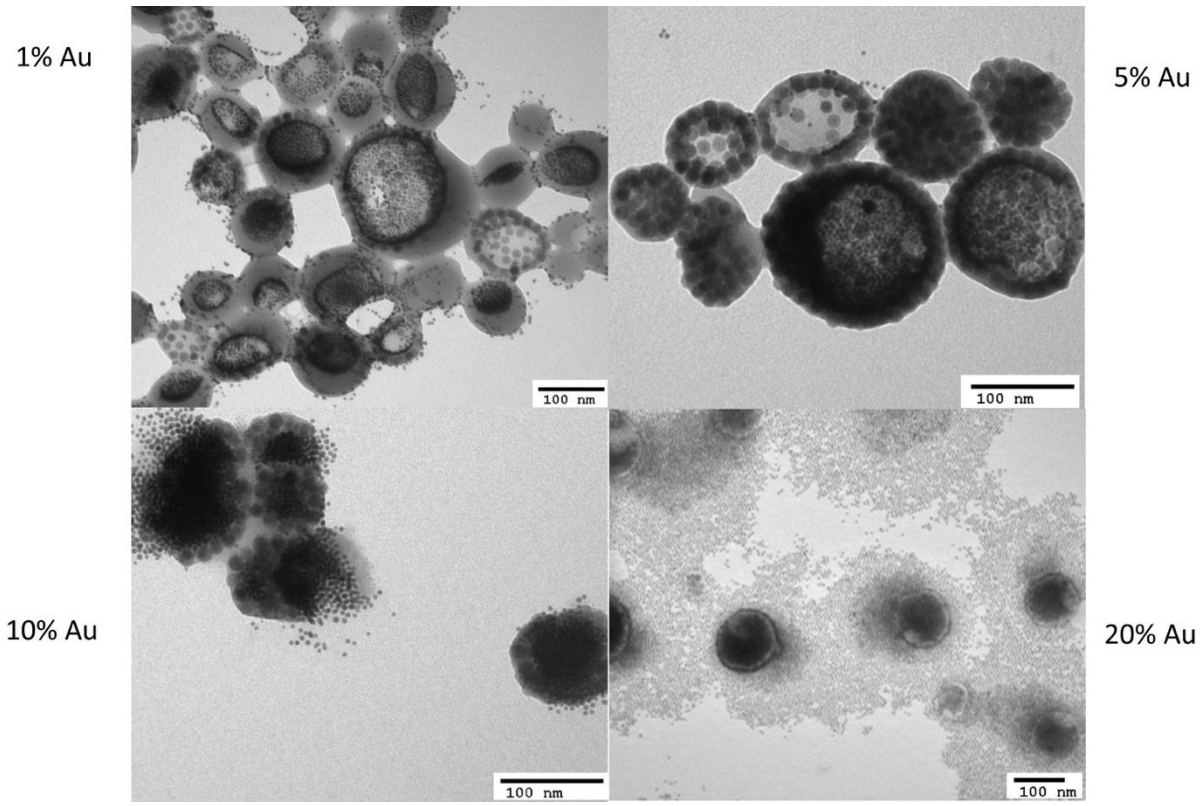

Figure S5. TEM images show the different number of AuNP and IONP and structural differences of JNS formed from different ratios of AuTCM and FeTCM. The percentage of AuNP in AuTCM was varied as indicated in the Figure. 1% and 5% of AuTCM yielded uncompleted JNS and FeBL were found in the product after purification. While 20% AuNP in AuTCM show over excessive AuNP that are unreacted to FeTCM and free TCM resulting in releasing single AuNPs and cause precipitation. 10% AuNP in AuTCM represent the optimal JNS nanostructures as there is neither unreacted AuNP nor FeBL appearing in TEM images.

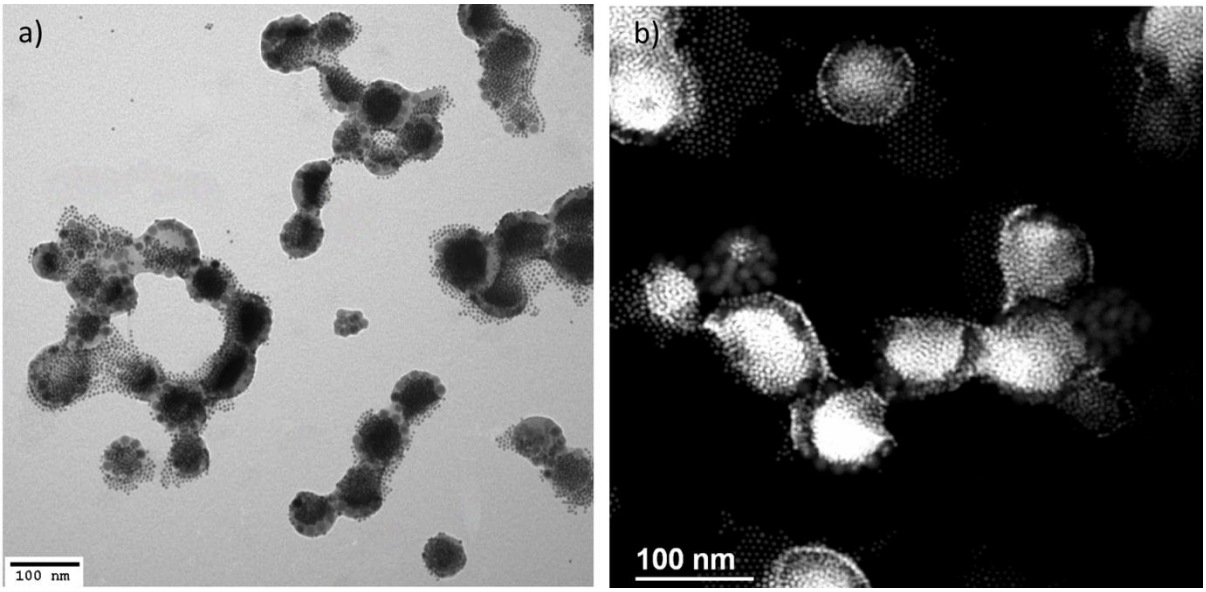

Figure S6. a) and b) represent a TEM and STEM-HADDF image of JNS showing that multiple AuNP and IONP are combined together as a single entity regardless of their orientation under the TEM and STEM. Darker tiny dots under TEM image and brighter spots under STEM image indicates AuNPs. The big grey spheres under TEM image and dark sphere under STEM represent IONPs.

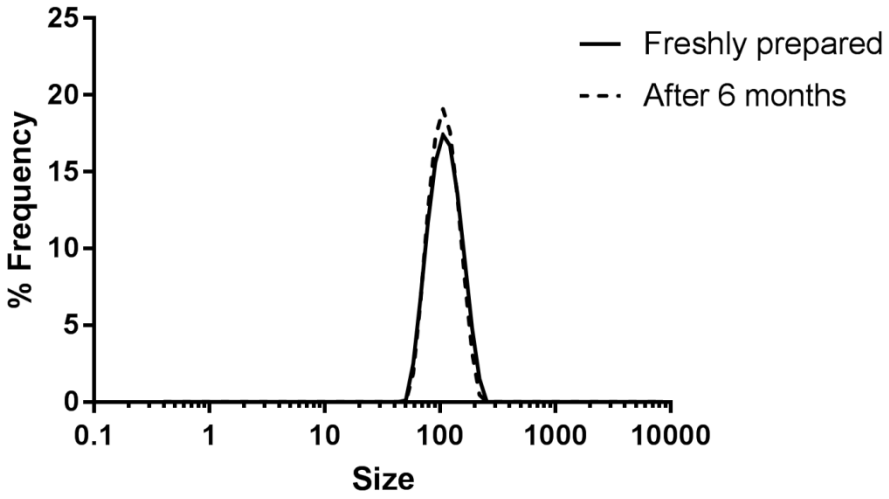

Figure S7. DLS data indicate JNS are stable over a period of 6 months after being stored at 4 °C. There is no change in hydrodynamic diameter.

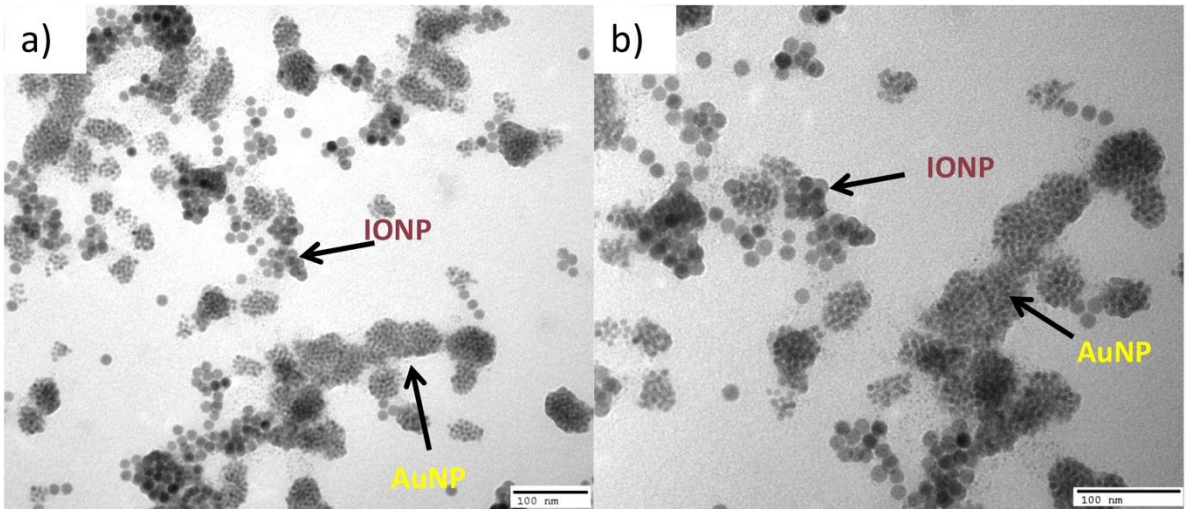

Figure S8. TEM images of the mixture of 5 nm AuNPs encapsulated in non-TCM (PS-*b*-PEO) and 15 nm IONPs loaded in non-TCM before (a) and after (b) 3 hours of high temperature treatment with free non-TCM seeds. The data suggest that there was no JNS formation. These two types of NP-TCMs remained separated in the solution. Scale bars are 100 nm.

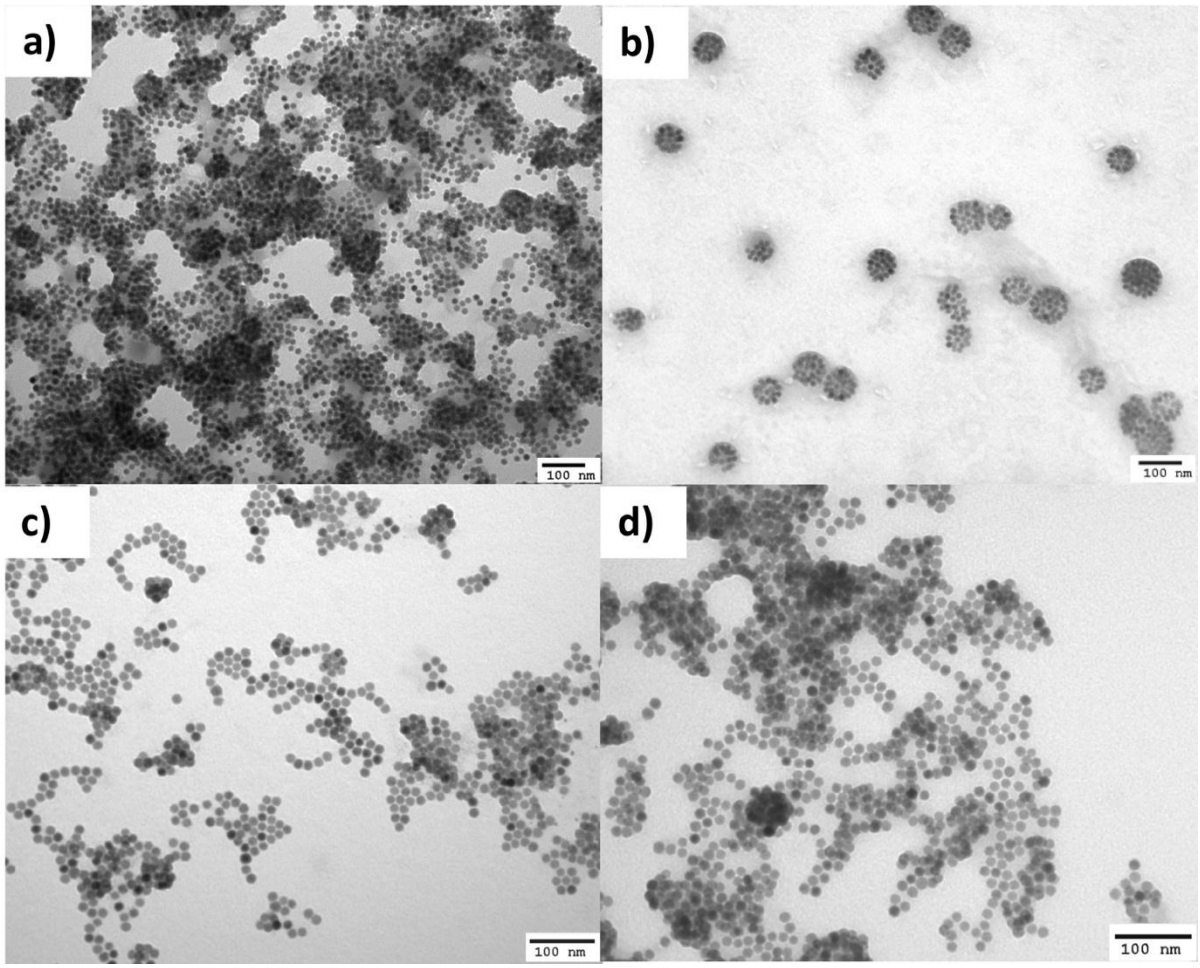

Figure S9. TEM images of FeTCMs before (a) and after (b) heat trigger. Morphological transformation of FeTCM is clearly observed under TEM. The cluster FeTCMs can undergo self-assembly and form FeBL. (c) and (d) show TEM images of nonFeTCMs before and after heat trigger respectively. No structural transformation was observed.

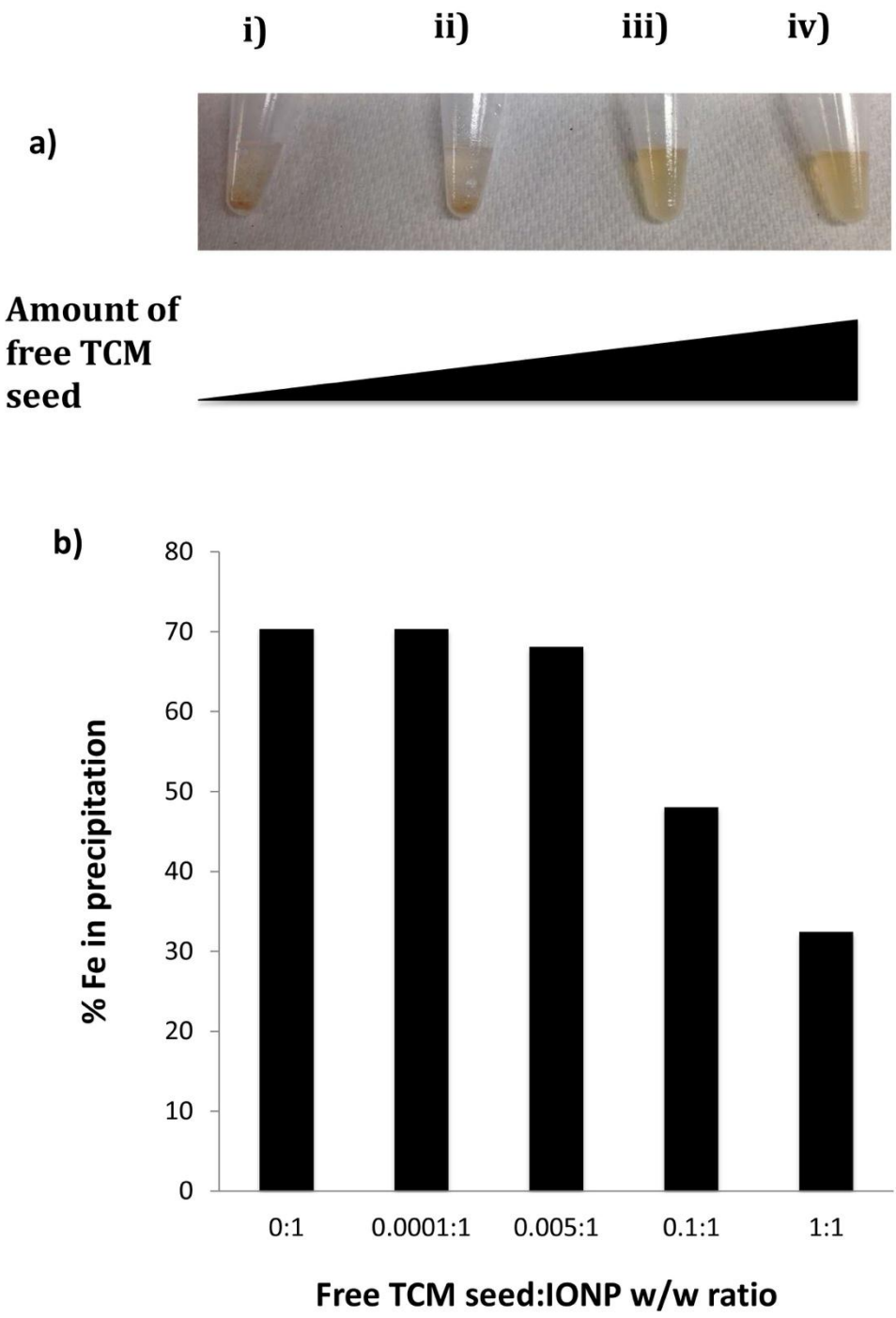

Figure S10. (a)Top panel shows that IONPs were released from the micelles and precipitated in the aqueous media. The amount of precipitation is inversely proportional to the amount of free

TCM seeds. (b)The bottom chart shows percentage of iron precipitation released from the

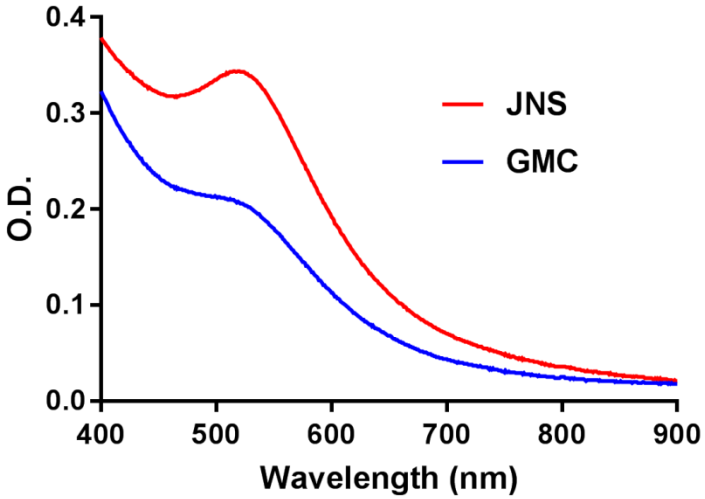

micelles at different weight ratios of the TCM seed with the fixing amount of IONPs (1mg).

Figure S11. Absorption spectrum of JNS and GMC at the same concentration of Au and Fe. JNS show overall stronger absorption than GMC. The maximum absorptions of JNS and GMC are 520 nm and 504 nm respectively.